9th AIAA/ASME Joint Thermophysics dan Heat Transfer Conference, 5-8 Jun 2006, San Francisco, California

Identification of microscale ablative properties of C/C composites using inverse simulation

Yvan Aspa and Michel Quintard
Institut de Mécanique des Fluides, Toulouse, FRANCE

Jean Lachaud and Gérard L. Vignoles
Laboratoire des Composites Thermostructuraux, Pessac, FRANCE

The objective of this work is to obtain, by an inverse approach, the reactivity of micro-scale components of ablative C/C composites. A model has been built for micro-scale ablation and a has been numerically implemented using a VOF method. The application of the approach is illustrated by the identification of reactivities from recession data and SEM observation of the ablated composite surface.

Nomenclature

a	Order of the kinetic law
A	Pre-exponential factor for recession velocity, kg/m^2/s/atm^{-a}
C	CO_2 Concentration, mol/m^3
D	CO_2 Diffusion coefficient, m^2/s
E_a	Activation energy, kcal/mol
h	Diffusive layer thickness, m
k	Reactivity, m/s
K	Pre-exponential factor for reactivity, m/(s K)
M	Molar mass, kg/mol
T	Temperature, K
V_a	Recession velocity, m/s
x	Normalized concentration
ρ	Density, kg/m^3
υ	Molar volume, m^3/mol

Subscript

0	Top domain boundary
f	Fiber property
i	Interphase property
m	Matrix property
ox	Gaseous oxidant
s	Solid property

I. Introduction

Composite materials are heterogeneous multiscale media. For them homogenized laws for effective behavior prediction are well established and largely used in structural mechanics. It is not the case for the

heterogeneous chemical reactivity especially in gasification processes.
The causes of the yet limited development of such approaches are both theoretical and practical. On one hand, theoretical tools for homogenization of reactive heterogeneous surfaces are rather recent.[1–3] Moreover, they consider reactive but non-recessive surfaces which is a strong limitation to their application to materials with a receding surface, like ablative C/C composites. On the other hand, the studies are limited in their application to CMC because the elementary reactivities are often unknown. For instance, it is difficult to obtain a stand-alone matrix identical to the surrounding fiber one because of fiber-matrix interaction during matrix elaboration.
Our study aims at identifying elementary reactivities of ablative C/C composites. In order to obtain those reactivities, a model for micro-scale ablation is set up, numerical simulation code is build. Basing on this code an inverse simulation fed with experimental data is performed.

A. Background

Carbon/Carbon composites (C/C) are among the few materials that are able to withstand the conditions inherent to new solid-propellant generations. Indeed, they combine a good ratio high temperature mechanical properties to density.
When exposed to flow, C/C are attacked by the solid-propellant gaseous products. This attack causes a surface recession and a morphological deformation of the throat. This phenomenon which groups several causes (mechanical erosion, gasification,...) is called *ablation*. The recession modifies the mass transport in gas phase as heat flow in both phases introduces a strong coupling between the evolution of the solid and the dynamical behavior of the fluid.
Ablation has two negative effects :

- During motor operation, the throat section increases, causing a loss of performance;
- The thickness of the C/C part reduces, increasing the heat flow received by weak parts.

However, as the phenomenon of ablation is globally endothermal, gasification of C/C consumes a non-negligible amount of heat, ensuring a thermal protection to the weak parts.
Considering all these effects, it is understood that nozzle design has to take ablation into account.

B. Micro-scale description

1. *Phenomenology*

At throat level, the Mach number of gases equals unity. In typical conditions, the pressure is close to 5 MPa and the temperature reaches 3000 K^4 . Inside the concentration layer, species diffuse to the wall and cause the surface ablation, mainly by oxidation according to the two following heterogeneous reaction balances:[4,5]

$$C_{(s)} + H_2O \rightarrow CO + H_2 \quad (1)$$
$$C_{(s)} + CO_2 \rightarrow 2\,CO \quad (2)$$

Accordingly, there exists a backward diffusion of the oxidation products : CO et H_2. As a matter of fact, the chemistry is somewhat more complicated, due to the existence of radical species, but Eqs. (1-2) are sufficient to describe what happens in the present purpose.
In typical solid propellants, the combustion products also contain aluminium particles. However, in the studied nozzles, most of these particles are rejected out of the boundary layers and do not reach appreciably the surface. Therefore, in the following study, focused on wall effects, the multiphasic character of the flow is ignored.

2. *Material*

The presently studied material is a C/C composite, manufactured by Snecma Propulsion Solide (SAFRAN group) formerly SEP, named SepCarb® 4D. This material has a three-dimensional structure with four reinforcement directions.[6] The reinforcement directions are parallel to the four larger diagonals of a cube as described in figure 1. The reinforcing material is made of bundles of carbon fibers in a carbon matrix. The diameter of these bundles varies typically between 1 and 3 mm.[6]

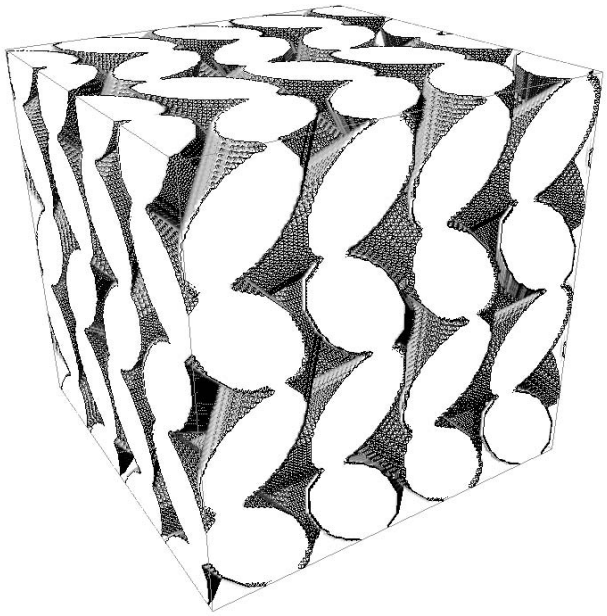

Figure 1. 4D architecture

II. Model set up

A. Material recession model

At micro-scale, the reinforcements can be described by a periodic array of parallel fibers. These fibers are surrounded by an interphase and a matrix. The bundles are described by a periodic unit cell describing the elementary pattern of the material. Each component is modeled by a homogeneous isotropic phase having is own reactivity.
For small variations of the throat nozzle section, the boundary layers do not grow. The top of the boundary layers recedes with the surface. Therefore, the evolution of the composite is studied in a local frame following the mean movement of the surface.

B. Kinetics Model

A literature review has been conducted to investigate the reaction kinetics of carbon with the gaseous form of H_2O and CO_2 at high temperatures. Sets of heterogeneous reaction kinetics were obtained for various graphites[7–9] with stagnation point studies. A kinetic law for 4D was obtained in nozzle throat configuration.[10] All these studies are considering the specific rates of the both reactions Eq. 2 and Eq. 1 to be equal except *Chelliah et al.*[7] in which kinetics are different, though rather equivalent from one reaction to the other. The kinetics are summarized under a coherent form in the table 1.

A first-order kinetic is given by each author except by *Chelliah et al.*[7] The fractional order observed in this case could be caused by diffusional limitations at high temperatures.
The reactivity k of the component is locally defined by :

$$V_a = \upsilon_s \, k \, C \tag{3}$$

with υ_s the molar volume of the solid. From the law given at table 1, k is identified to :

$$k = \frac{A \, R}{M_c} T_s \, e^{-E_a/RT_s} \tag{4}$$

$$V_a = \frac{A}{\rho_s} p_i^a e^{-E_a/RT_s}$$

Source	$A\ (kg.m^{-2}s^{-1}atm^{-a})$	a	$E_a\ (kcal/mol)$
[10] Frozen BL	$4.25 - 4.48\ 10^6$	1	20.07
[10] Eq. BL	$2.12 - 2.23\ 10^6$	1	18.52
[7] H_20	$4.8\ 10^5$	0.5	68.8
[7] CO_2	$9.0\ 10^5$	0.5	68.1
[8]	$2.43\ 10^3$	1	41.9
[9]	158	1	40

Table 1. Kinetics given by the literature

where M_c is the molar mass of the solid. One must note that, considering the experimental difficulties and the variety of carbon-based studied materials, the kinetic data are little dispersed. At a given temperature from 2000 K to 3000 K, the ratio between the upper and lower boundaries given by table 1 is between 10 and 50.

C. Heat and mass transfer

In typical ablation conditions, the composite surface receives a total heat flux of 10 $MW.m^{-2}$.[10] At high temperature, the composite conductivity is about 50 $W.m^{-1}K^{-1}$.[10] This gives a maximal thermal gradient of approximatively 0.2 $K.\mu m^{-1}$. As consequence, the system will be considered isothermal at micro-scale.
In the concentration boundary layer, mass transport is mainly driven by the eddies. Turbulent diffusivity is several times greater than the laminar diffusivity in the turbulent core. In this zone the mole fractions are rather uniform. Therefore, the appearing diffusive layer is very thin. This promotes a recession mechanism essentially limited by surface kinetics.
Some assumptions are added to these considerations in order to set up the mass transfer model. They are :

- the pressure gradients are negligible due to the small scale of the system ;
- the oxidation chemistry is restricted to eq. (2) with an assumed first order kinetic law ;
- CO and CO_2 are the only two considered species. The mass transport reduces then to simple binary diffusion, and the CO partial pressure is simply calculated from the CO_2 partial pressure by pressure conservation ;

Moreover, an additional relation between the the boundary thickness evolution and the surface roughness is needed. In this paper, on the basis of averaging considerations, it is assumed that, during surface recession, the mean boundary layer thickness is conserved.
With such assumptions, only two mass balances are necessary for the model, one for the solid (described by its interface $z = h(x, y, t)$) and one for CO_2 molar concentration C. With suited boundary conditions, the full set of equations to be solved is:

$$C = C_0 \quad \text{as top boundary condition} \tag{5}$$
$$\partial_t C = \nabla \cdot (D\underline{\nabla C}) \quad \text{in the fluid} \tag{6}$$
$$(-D\underline{\nabla C}) \cdot \underline{n} = -k\ C \quad \text{at the fluid-solid interface } (z = h) \tag{7}$$
$$\partial_t h + \langle \partial_t h \rangle = -\upsilon_s k C \underline{n}.\underline{e_z} \quad \text{at the fluid-solid interface } (z = h) \tag{8}$$

where the following quantities have been introduced : D is the diffusion coefficient, k is the material-dependent heterogeneous reaction constant, and h the local boundary layer height. Maintaining the interface at a constant altitude implies the use of the second term on the left-hand side of eq. (8), which is an average recession velocity.
The obtained model is schematized in figure 2.

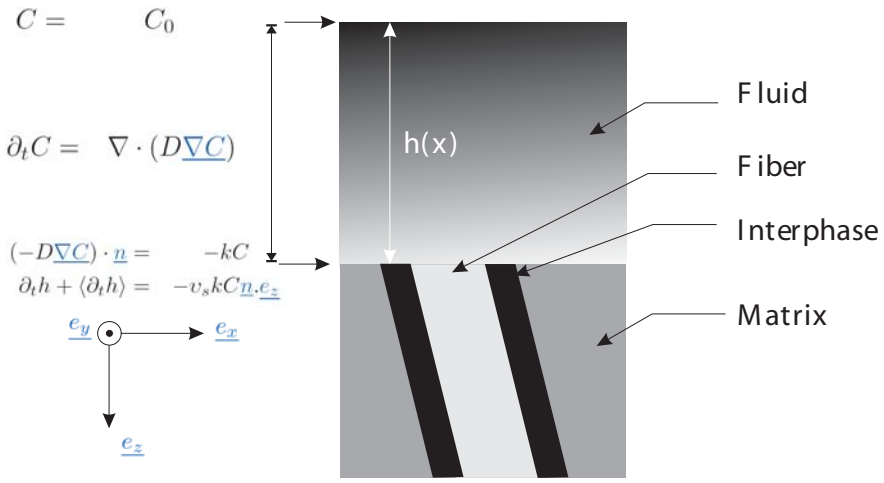

Figure 2. Sketch of the microscale ablation model

III. Numerical Simulation Code

A. Numerical method

The problem solutions have been sought in $3D$, on a fixed regular grid, which has the advantage of a very simple treatment of bulk regions far from interface. Moreover, such a grid avoids any time-expensive mesh refinement procedure. Several methods are available to convert the mathematical problem into continuous form. In this work, the chosen method is the VOF[11] (Volume Of Fluid) method which uses a Eulerian description.
In each elementary volume, a phase indicator variable ε_s is used. This variable is defined by the local volume fraction of solid. The transfer equations are discretized on a regular cartesian mesh following a finite volume scheme. At elementary volume scale, the interface is locally represented by a plane (PLIC method[12]). Each elementary volume surface Ω is the locus of matter exchange between fluid/fluid interfaces at shared sides and solid/fluid ones at the inner solid/fluid interface. To model properly the fluxes, these exchange surfaces are evaluated at each time-step. The basis of this computation is exposed by Scardovelli.[13]
The global algorithm loop is the following :

1. The elementary surfaces are computed ;
2. The diffusion-reaction problem is solved ;
3. The surface is ablated.

The variables C and ε_s have been partially uncoupled. This operation has a negligibly impact on the results because the evolution of concentration field is several times faster than the morphological evolution of the surface.

B. Validation

The numerical code DiAbl3D regroups several routines which are coupled in the considered physical model. The morphological evolution engine was validated with the evolution of spheres in uniform concentration fields.
In order to validate the concentration field computation, a non-recessive surface has been taken. Several configurations have been computed in DiAbl3D and compared with commercial FEM codes. An example of such a comparison is given at figure 3. The simulated system is a unit side square with a crenel. The sides of the crenel have a reactivity equal to 10, the base a reactivity equal to 1. The diffusion coefficient is set equal to unity. The concentration fields obtained in fluid sections are compared between the two codes. The mesh of the FEM is shown on the top of figure 3. A 100^2 regular grid was used in DiAbl3D . The bottom graphs shows a very good agreement between the two methods.

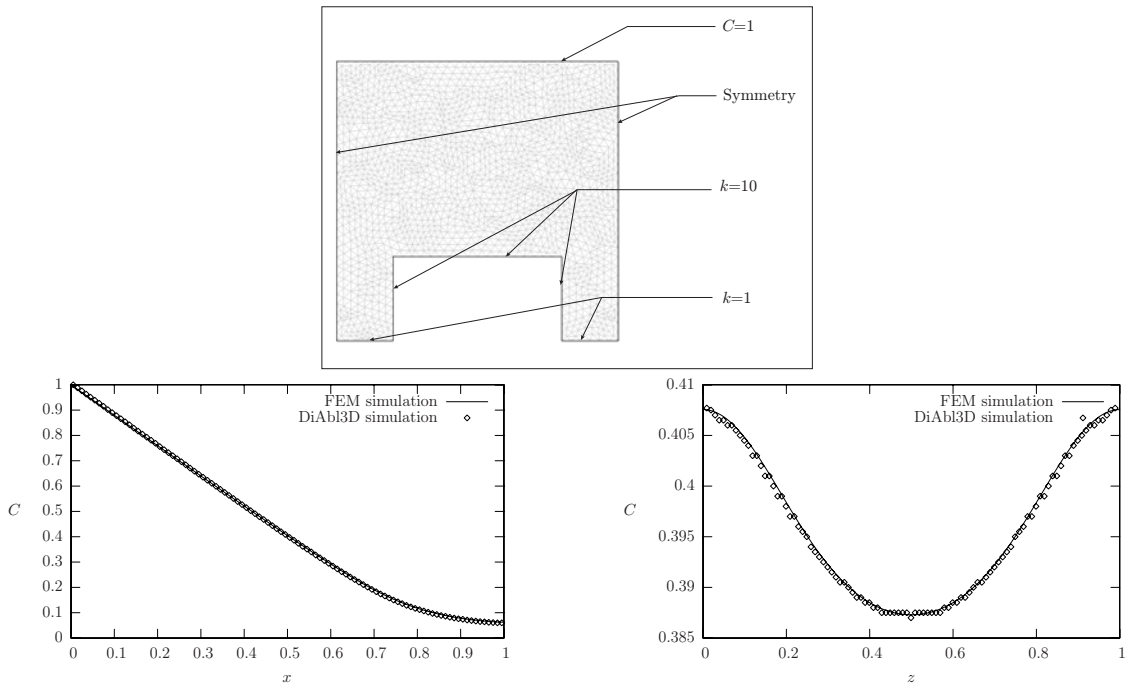

Figure 3. Comparison between concentration values computed by DiAbl3D and Femlab©on vertical and horizontal sections

C. Example of simulation

To illustrate the simulation of a simple material pattern, a single fiber is surrounded by a more reactive matrix, without a third solid phase. The simulation in a reaction-controlled case with a contrast $\tilde{k} = \frac{k_m}{k_f} = 7$ is given figure 4.

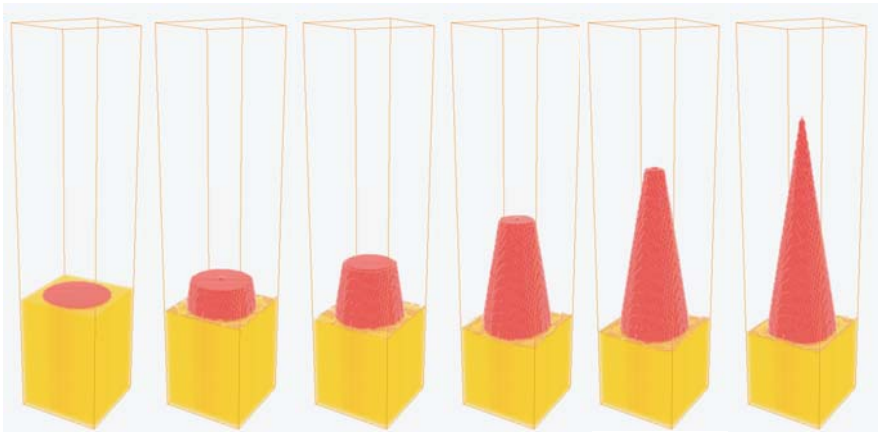

Figure 4. Evolution of a simple material pattern

During first times, the matrix, which is more reactive, lets the fiber emerge. The fiber tip is ablated by the sides acquiring a conical steady-state morphology. At this moment, each surface point recede at the same velocity and the local slope is stationary. It is noted that in this case the cylindrical symmetry of the fiber is conserved during the evolution.

D. Effective behavior

The simulation gives the mean behavior of the material pattern in terms of consumed molar flux. The effective reactivity of the pattern is post-processed by the use of the following formula:

$$k_{eff} = \frac{1}{\frac{h}{D} - \frac{C_0}{J_{mol}}} \tag{9}$$

The maximum flux, given by the diffusion-controlled regime, is $J_{max} = \frac{D\,C_0}{h}$. This effective reactivity is a function of the reactivity of the phases. It is also influenced by the competition diffusion/reaction described by the Damköhler number : $Da = \frac{k\,h}{D}$.

IV. Inverse approach

To feed the inverse simulation and identify the elementary reactivities of the micro-scale components, data of ablation behavior are needed. Simulations are then ran in order to have the cloer results to experimental data.

A. Ablation data: Microscale Morphologies

Our approach uses the micro-scale morphology of the ablated composite as input of the inverse approach. These inputs are less influenced by the transfers in the turbulent boundary layer than the recession rate. Therefore they can be more easily described by a local model.

The SEM observation of the ablated materials reveals the roughness features of reinforcements at fiber-scale. The micrographs of figure 5 show the typical morphology at the center of the bundle. The fibers have an ogival profile with facets. The intra-bundle matrix seems to be preferentially oxidized. In fact, there are still parts of it, but they are difficult to distinguish from fiber tips. In order to find the residual of matrix, the edge of the reinforcement must be studied. In this zone the thickness of matrix is notably greater than in the core. The micrograph of figure 6 shows the aspect of the matrix. The analysis of this micrograph allows to understand that the weakest part of the reinforcement is a thin interphase surrounding the fibers. The role of this interphase in the oxidation of C/C composites has already been observed with other materials.[14] Furthermore, it can be seen at figure 6 that the slope of the edge of the fiber and the one of the matrix are similar. This indicates that their reactivities are equivalent. This leads to the following description of the material:

$$k_i \gg k_f \approx k_m \tag{10}$$

B. Simulations

A periodic unit cell with a geometrical arrangement of fiber, interphase and matrix similar to the actual bundle, with a fiber radius of 3 μm and an interphase thickness of 500 nm is built. Several simulations are ran to obtained the desired morphology. The equivalent morphology is elected by the optimization of the fiber tip angle in comparison of the one evaluated from observations to $\theta = 30° \pm 5°$. This angle has a rather large incertitude because of the difficulties inherent to the measure of an angle on 2D images of variables 3D objects. A better estimation would be obtained by the use of high-resolution X-ray tomographs.

1. 2D Simulations

Preliminary computations are made in 2D. The diffusion coefficient is set to $D = 10^{-4}\ m^2.s^{-1}$. The reactivities are initialized to $k_f = k_m = 10\ m.s^{-1}$ and $k_i = 60\ m.s^{-1}$. The steady-state morphology of this simulation is given at the center of figure 7. The effective reactivity is then $k_{eff} = 31.4\ m.s^{-1}$ and the top angle is identified to $\theta = 38°$. The global shape is not as angular as researched. This is due to the impact of diffusion limitations.

Such an effect is higher for faster reactions as seen at the bottom of figure 7 for $k_f = k_m = 30\ m.s^{-1}$ and $k_i = 180\ m.s^{-1}$. It can be noted that, as seen for non recessive surfaces,[2,3] that the mass transfer limitation also impacts the effective reactivity. Between the two preceding cases the elementary reactivities are tripled

when the effective reactivity is only doubled.
As the aimed morphology is very angular, reactivities are reduced. With $k_f = k_m = 1\ m.s^{-1}$ and $k_i = 6\ m.s^{-1}$, satisfying angle and global shape are obtained as seen at the center of figure 7. This couple of reactivities gives an effective reactivity equal to $k_{eff} = 5.26\ m.s^{-1}$. Reducing the reactivities and conserving the contrast leads to equivalent morphologies but non-realistic effective reactivities. Variations of contrast are shown on the first line of the figure 7 confirms the validity of the previous couple.
The 2D simulations have given an estimation of the reactivities as being close to : $k_f = k_m = 1\ m.s^{-1}$ and $k_i = 6\ m.s^{-1}$. Moreover, such values agrees with experimental value of $4 - 11\ m.s^{-1}$ obtained from recession rate analysis.[4]
To verify these choice of reactivity, 3D simulation is driven.

2. 3D Simulation

As observed of SEM micrographs, fibers show facets. In order to obtain this morphology and to confirm the previously assumed reactivities, 3D simulations are ran. The elementary pattern is made of $(1, 1, 1)$ direction parallel fibers. The dimensions are the same as 2D unit cell. The reactivities are chosen equal to $k_f = k_m = 1\ m.s^{-1}$ and $k_i = 6\ m.s^{-1}$.
The evolution of the unit cell is presented at figure 8. As expected the surface reaches a pointed steady-state morphology. The obtained pattern moves in the mean plane following a (1,1,0) direction without any deformation. It can be noted that due to the inclination, the fiber tip loses its revolution symmetry and shows facets. The mean top angle is globally conserved regarding 2d simulations.
On the figure 10(a), the reconstruction by repetition of the elementary pattern. The similitude with the SEM micrographs figure 5 confirms the validity of our approach. The figure 10(b) presents the diffusion streamlines colorized by the normalized concentration $x = \frac{C}{C_0}$.

V. Conclusion

The micro-scale ablation of C/C composites has been described. Basing on domain dimension, a simple model was built. A numerical code was was implemented to simulate the recession of heterogenous surfaces. The code was then used to obtain, in an inverse approach, the elementary reactivities of the composite.
It was found that at microscale, the weakness of the composite reinforcement is the thin interphase surrounding the fibers. The identified effective reactivity of the composite agreed with the literature data. The fibers and the matrix were found to have comparable reactivities, while the interphase is six times more reactive. The approach detailed in this paper is transposable to others applications of C/C showing the same micro-morphology has illustrated by figure 11. To be extended to the upper scales, the physics of the model has to be completed (turbulent flow and heat coupling, multi-component aspect).

Acknowledgments

The authors wish to thank Snecma Propulsion Solide for Y.A. PhD grant and CEA for Y.A. PhD grant. C. François (Snecma) is also acknowledged for her support in SEM manipulation.

References

[1]Juhasz, N. M. and Deen, W. D., "Effect of local Peclet number on Mass Transfer to a Heterogeneous Surface," *Ind. Eng. Chem. Res.*, Vol. 3, 1991, pp. 556,562.

[2]Wood, B., Quintard, M., and Whitaker, S., "Jump Conditions at Non-Uniform Boundaries: The Catalytic Surface," *Chemical Engineering Science*, Vol. 55, 2000, pp. 5231–5245.

[3]Valdes-Parada, F. J., Goyeau, B., and Alberto Ochoa-Tapia, J., "Diffusive mass transfer between a microporous medium and an homogeneous fluid: Jump boundary conditions," *Chemical Engineering Science*, Vol. 61, No. 5, March 2006, pp. 1692–1704.

[4]Borie, V., Brulard, J., and Lengellé, G., "An aerothermochemical analysis of Carbon-Carbon nozzle regression in solid-propellant rocket motors," *24th Joint Propulsion conference*, AIAA/ASME/SAE/ASEE, Boston, MA, July 1988.

[5]Kuo, K. and Keswani, S., "A Comprehensive Theoretical Model for Carbon-Carbon Composite Nozzle Recession," *Combustion Science and Technology*, Vol. 42, 1986, pp. 177–192.

[6]Aubard, X., Cluzel, C., Guitard, L., and Ladeveze, P., "Modelling of the mechanical behaviour of 4D carbon/carbon composite materials," *Composites Science and Technology*, Vol. 58, No. 5, 1998, pp. 701–708.

[7]Chelliah, H. K., Makino, A., Kato, I., Araki, N., and Law, C. K., "Modeling of graphite oxidation in a stagnation-point flow field using detailed homogeneous and semiglobal heterogeneous mechanisms with comparisons to experiments," *Combustion and Flame*, Vol. 104, No. 4, March 1996, pp. 469–480.

[8]Libby, P. A. and Blake, T. R., "Burning carbon particles in the presence of water vapor," *Combustion and Flame*, Vol. 41, 1981, pp. 123–147.

[9]Golovina, E. S., "The gasification of carbon by carbon dioxide at high temperatures and pressures," *Carbon*, Vol. 18, 1980, pp. 197–201.

[10]Borie, V., Maisonneuve, Y., Lambert, D., and Lengellé, G., "Ablation des matériaux de tuyères de propulseurs à propergol Solide," Tech. Rep. 13, ONERA, nov 1990.

[11]Guyeyffier, D., Li, J., Nadim, A., Scardovelli, R., and Zaleski, S., "Volume-of-Fluid Interface Tracking with Smoothed Surface Stress Methods for Three-Dimensional Flows," *Journal of Computational Physics*, Vol. 152, 1999, pp. 423–456.

[12]Welch, S. W. J. and Wilson, J., "A Volume of Fluid Based Method for Fluid Flows with Phase Change," *Journal of Computational Physics*, Vol. 160, 2000, pp. 662–682.

[13]Scardovelli, R. and Zaleski, S., "Analytical Relations Connecting Linear Interfaces and Volume Fractions in Rectangular Grids," *Journal of Computational Physics*, Vol. 164, 2000, pp. 228–237.

[14]Labruquère, S., Bourrat, X., Pailler, R., and Naslain, R., "Structure and oxidation of C/C composites: role of the interface," *Carbon*, Vol. 39, 2001, pp. 971–984.

[15]Pestchanyi, S. and Wuerz, H., "3-D simulation of macroscopic erosion of CFC under ITER off-normal heat loads," *Fusion Engineering and Design*, Vol. 66, 2003, pp. 271–276.

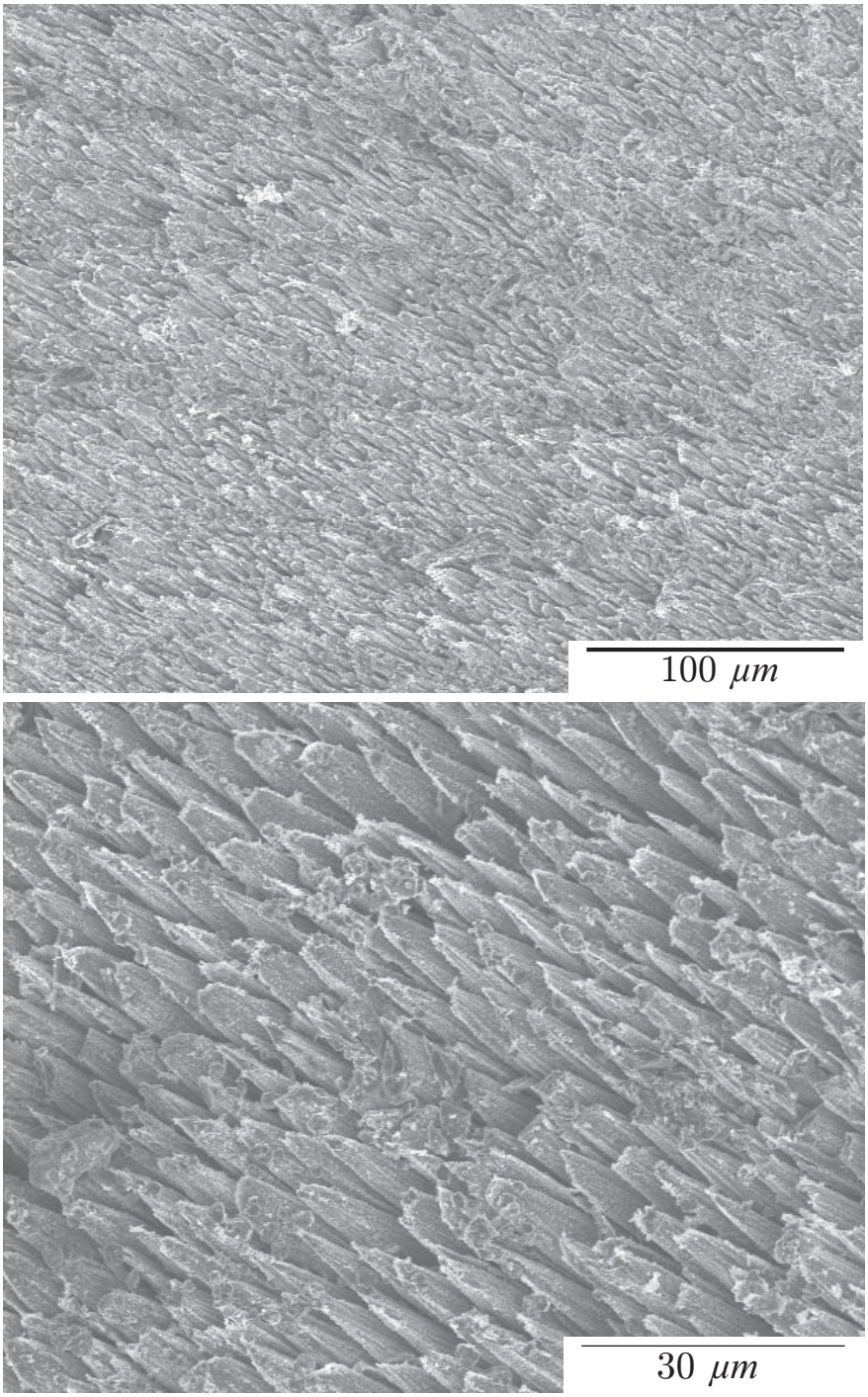

Figure 5. SEM micrograph of ablated fibers at bundle core

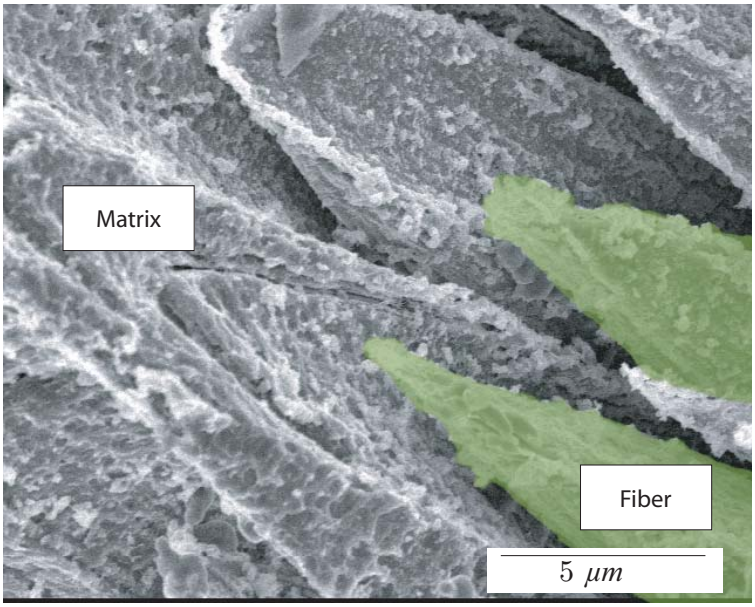

Figure 6. SEM micrograph of ablated fibers at bundle edge

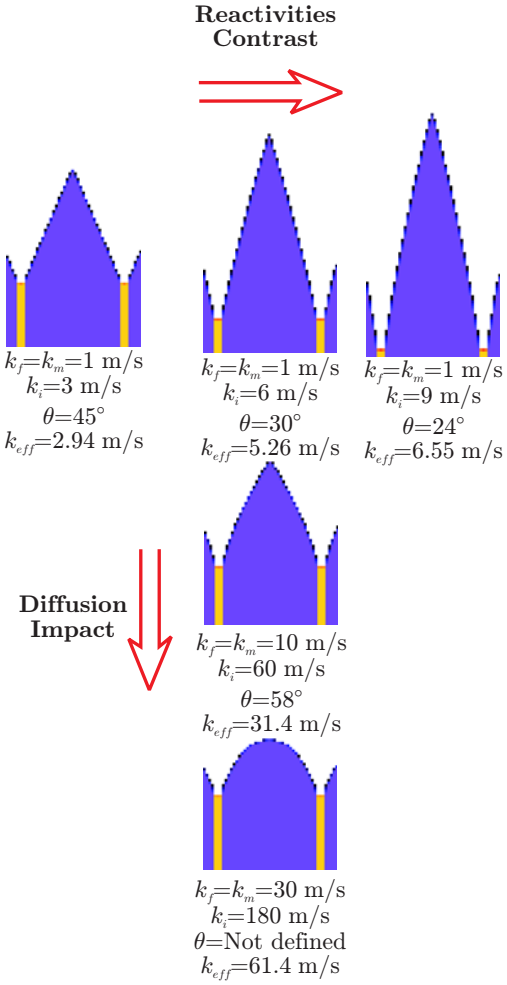

Figure 7. 2D Simulations: steady-state morphologies and numerical parameters

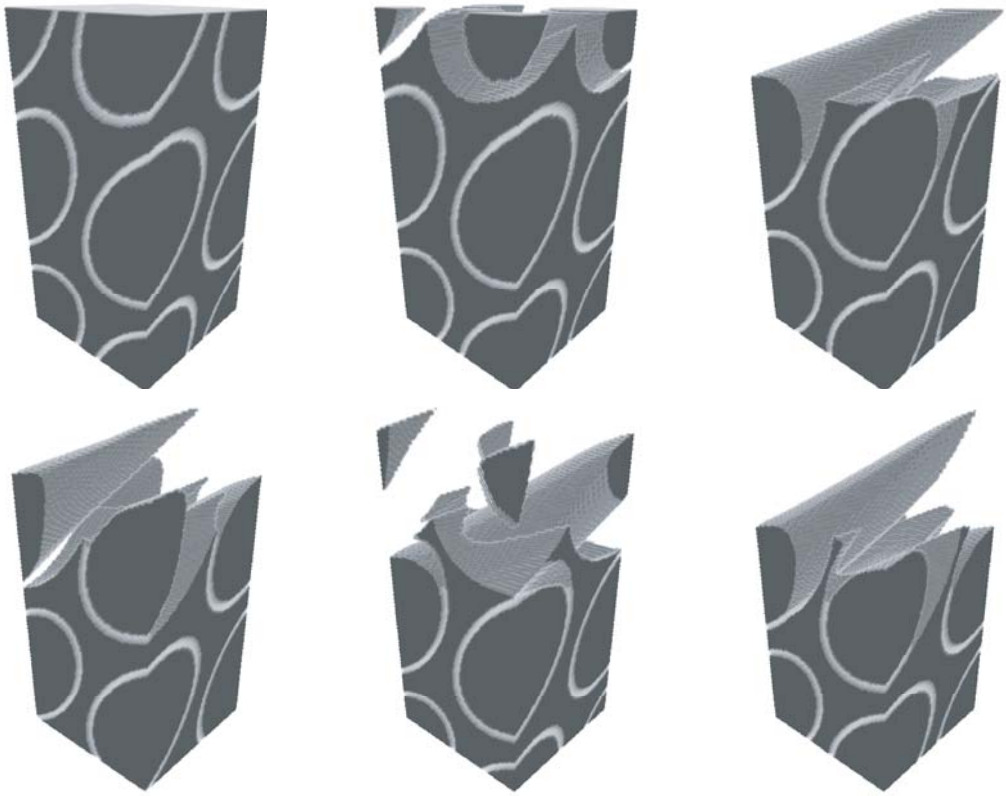

Figure 8. 3D Simulation: Evolution of the unit cell

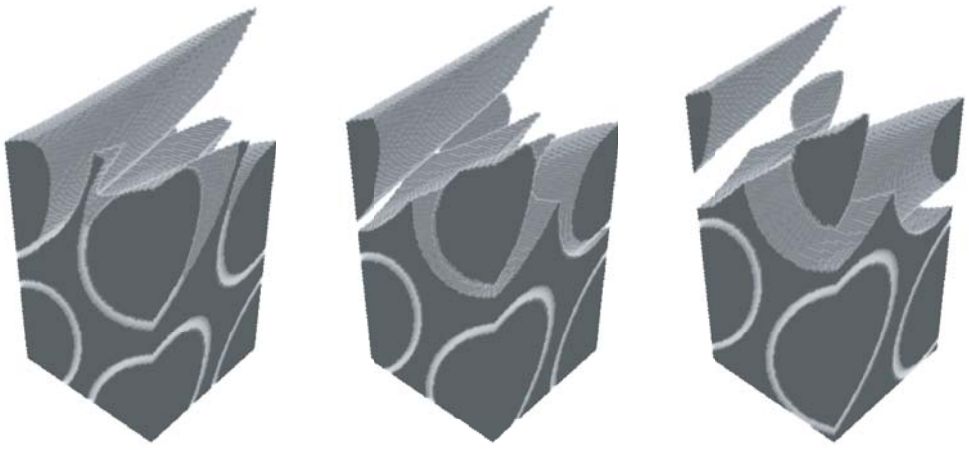

Figure 9. 3D Simulation: plane movement of the steady-state morphology

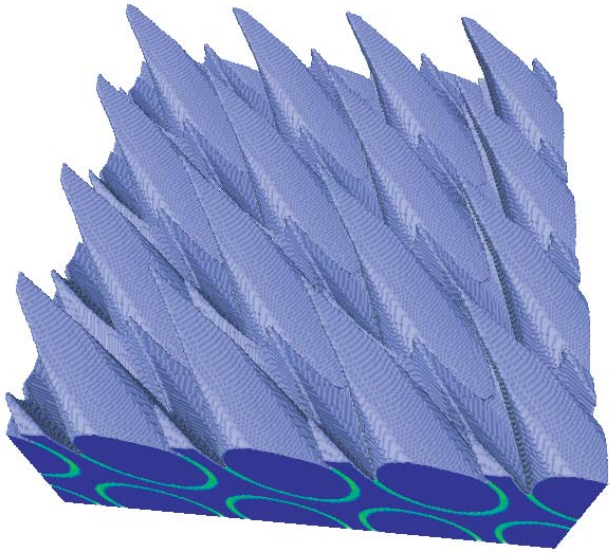

(a) ***Surface reconstruction.***

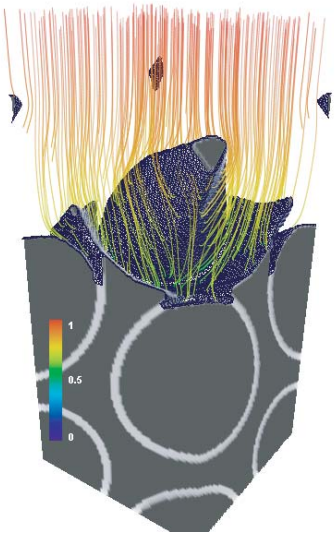

(b) ***Diffusion streamlines colorized by*** $x = C/C_0$.

Figure 10. Reconstruction of the composite surface and diffusion streamlines for stationary morphology

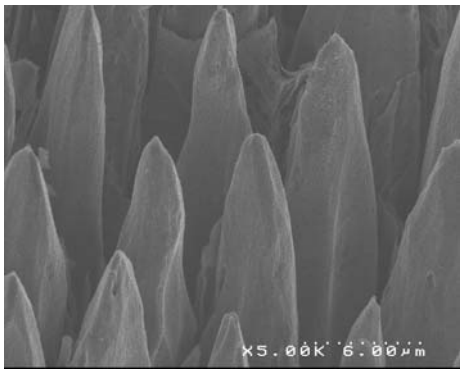

(a) ***Reentry Body***

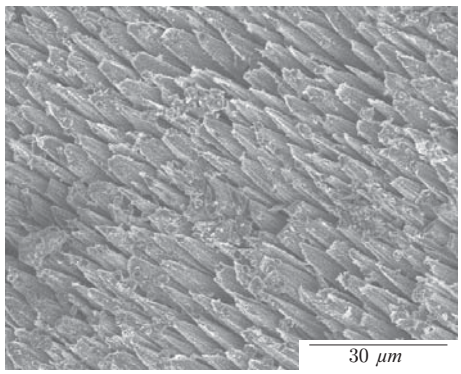

(b) ***Nozzle***

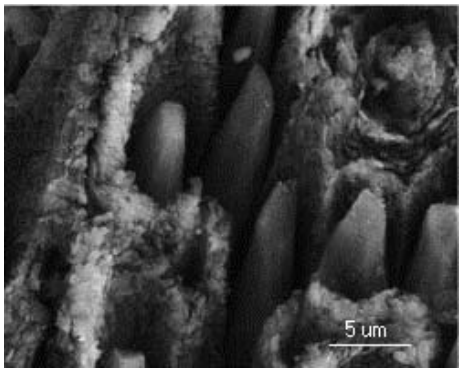

(c) ***Fusion Tokamak***

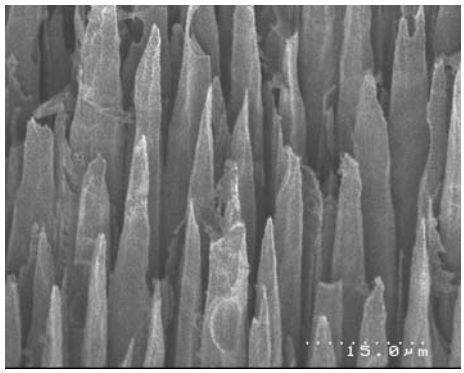

(d) ***Oxidation furnace***

Figure 11. C/C ablated composites micrographs